



HAL
open science

Low BCL-xL expression in triple-negative breast cancer cells favors chemotherapy efficacy, and this effect is limited by cancer-associated fibroblasts

Lisa Nocquet, Julie Roul, Chloé C Lefebvre, Laurine Duarte, Mario Campone, Philippe P Juin, Frédérique Souazé

► To cite this version:

Lisa Nocquet, Julie Roul, Chloé C Lefebvre, Laurine Duarte, Mario Campone, et al.. Low BCL-xL expression in triple-negative breast cancer cells favors chemotherapy efficacy, and this effect is limited by cancer-associated fibroblasts. *Scientific Reports*, 2024, 14 (1), pp.14177. 10.1038/s41598-024-64696-z. hal-04618775

HAL Id: hal-04618775

<https://hal.science/hal-04618775>

Submitted on 20 Jun 2024

HAL is a multi-disciplinary open access archive for the deposit and dissemination of scientific research documents, whether they are published or not. The documents may come from teaching and research institutions in France or abroad, or from public or private research centers.

L'archive ouverte pluridisciplinaire **HAL**, est destinée au dépôt et à la diffusion de documents scientifiques de niveau recherche, publiés ou non, émanant des établissements d'enseignement et de recherche français ou étrangers, des laboratoires publics ou privés.



OPEN

Low BCL-xL expression in triple-negative breast cancer cells favors chemotherapy efficacy, and this effect is limited by cancer-associated fibroblasts

Lisa Nocquet^{1,2,3}, Julie Roul^{1,2,3,4}, Chloé C. Lefebvre^{1,2,3}, Laurine Duarte^{1,2,3}, Mario Campone^{1,3,4}, Philippe P. Juin^{1,2,3,4}✉ & Frédérique Souazé^{1,2,3}✉

Triple negative breast cancers (TNBC) present a poor prognosis primarily due to their resistance to chemotherapy. This resistance is known to be associated with elevated expression of certain anti-apoptotic members within the proteins of the BCL-2 family (namely BCL-xL, MCL-1 and BCL-2). These regulate cell death by inhibiting pro-apoptotic protein activation through binding and sequestration and they can be selectively antagonized by BH3 mimetics. Yet the individual influences of BCL-xL, MCL-1, and BCL-2 on the sensitivity of TNBC cells to chemotherapy, and their regulation by cancer-associated fibroblasts (CAFs), major components of the tumor stroma and key contributors to therapy resistance remain to be delineated. Using gene editing or BH3 mimetics to inhibit anti-apoptotic BCL-2 family proteins in TNBC line MDA-MB-231, we show that BCL-xL and MCL-1 promote cancer cell survival through compensatory mechanisms. This cell line shows limited sensitivity to chemotherapy, in line with the clinical resistance observed in TNBC patients. We elucidate that BCL-xL plays a pivotal role in therapy response, as its depletion or pharmacological inhibition heightened chemotherapy effectiveness. Moreover, BCL-xL expression is associated with chemotherapy resistance in patient-derived tumoroids where its pharmacological inhibition enhances *ex vivo* response to chemotherapy. In a co-culture model of cancer cells and CAFs, we observe that even in a context where BCL-xL reduced expression renders cancer cells more susceptible to chemotherapy, those in contact with CAFs display reduced sensitivity to chemotherapy. Thus CAFs exert a profound pro-survival effect in breast cancer cells, even in a setting highly favoring cell death through combined chemotherapy and absence of the main actor of chemoresistance, BCL-xL.

Keywords Apoptosis, Breast cancer, Cancer-associated fibroblasts, BCL-2 family, Chemotherapy

Triple negative breast cancer (TNBC), characterized by the lack of expression of hormonal receptors and the absence of Erb2 amplification, is associated with a poor prognosis due to its aggressive nature and the absence of effective targeted treatments. Consequently, TNBC treatment is often limited to non-targeted chemotherapy, which may not be sufficient to eliminate cancer cells^{1,2}. The limited effectiveness of therapy and the development of drug resistance in TNBC is in great part related to pathways regulating mitochondrial outer membrane permeabilization (MOMP). Many anticancer drugs commonly used in clinical practice rely on this mitochondria disrupting event to induce cancer cell death³. The BCL-2 family proteins play a crucial role in MOMP, which leads to the release of cytochrome c into the cytoplasm and the activation of a caspase cascade and subsequent cell death through canonical apoptosis or other cell death modes. Cancer cells can survive by altering the balance between anti-apoptotic and pro-apoptotic members of the BCL-2 family⁴. Numerous studies have demonstrated that elevated levels of pro-survival proteins, including BCL-xL, MCL-1, and BCL-2, are frequently observed in cancers and contribute to drug resistance⁵. BCL-xL and MCL-1 are notably overexpressed in TNBC cells compared to normal counterpart^{6–8}. BH3 mimetics, a class of small compounds, antagonize binding of BCL-2

¹INSERM, CNRS, CRCI2NA, Université de Nantes, 44000 Nantes, France. ²Equipe Labellisée LIGUE Contre le Cancer, Paris, France. ³SIRIC ILIAD, Nantes, Angers, France. ⁴ICO René Gauducheau, Saint Herblain, France. ✉email: philippe.juin@univ-nantes.fr; frederique.souaze@univ-nantes.fr

family anti-apoptotic proteins to pro-apoptotic proteins, creating an avenue to offset the excessive expression of these anti-apoptotic proteins⁴. These compounds present an opportunity to gain deeper insights into the exact mechanisms that contribute to chemoresistance. The effectiveness of BH3 mimetics depends on the expression and activity of pro-apoptotic BCL-2 family members and on the balance between the expression of the targeted anti-apoptotic proteins and non-targeted ones⁹. Pro-survival proteins can indeed compensate for each other by taking on released pro-apoptotic proteins induced by BH3 mimetics⁴.

The cancer stroma plays a significant role in cancer cell resistance to therapy¹⁰. CAFs in the tumor micro-environment have been reported to promote resistance to therapy in cancer cells through direct contacts or the local release of soluble factors^{11,12}. We previously showed that in luminal breast cancer, IL-6 secretion by CAFs mitigates the tumor BCL-2 dependency by inducing expression of cancer cell pro-survival protein MCL-1¹³.

In TNBC, identifying the specific pro-survival proteins involved in chemoresistance and investigating whether it is possible to sensitize cancer cells to chemotherapy when CAFs are present by targeting these factors is of particular interest to guide the development of therapeutic strategies. In our study, we used BH3 mimetics and gene silencing techniques to demonstrate the simultaneous and compensatory involvement of MCL-1 and BCL-xL in the survival of the TNBC cell line MDA-MB-231. Furthermore, our findings highlighted the role of the anti-apoptotic protein BCL-xL in mediating resistance to chemotherapy in TNBC. In a co-culture model, we revealed that even when the pro-survival effect of BCL-xL is disrupted, CAFs are still capable of significantly protecting TNBC cells from the effects of chemotherapy. Therefore, our study underscores the need to develop strategies to target CAFs and their interactions with TNBC cells in order to improve the efficacy of chemotherapy in TNBC.

Results

BCL-xL and MCL-1 are pivotal anti-apoptotic proteins responsible for the survival of MDA-MB-231 cell line

At first, we assessed the impact of various anti-apoptotic proteins from the BCL-2 family on the survival of MDA-MB-231 cell line. To achieve this, we generated silenced cells for MCL-1, BCL-xL, or BCL-2, designated as sg MCL-1, sg BCL-xL, and sg BCL-2, respectively, using a CRISPR-Cas9 based approach. Our findings revealed that MDA-MB-231 control line expressed all three anti-apoptotic proteins, albeit with low levels of BCL-2 (Fig. 1A). Western blot analysis corroborated that MDA-MB-231 sg BCL-xL, sg MCL-1, and sg BCL-2 cells exhibit a deficiency in BCL-xL, MCL-1, and BCL-2, respectively (Fig. 1A).

Subsequently, we investigated the effects of both loss and pharmacological inhibition of BCL-xL, MCL-1, or BCL-2 on the survival of MDA-MB-231 (Fig. 1B). In control cell lines, only the pharmacological inhibition of

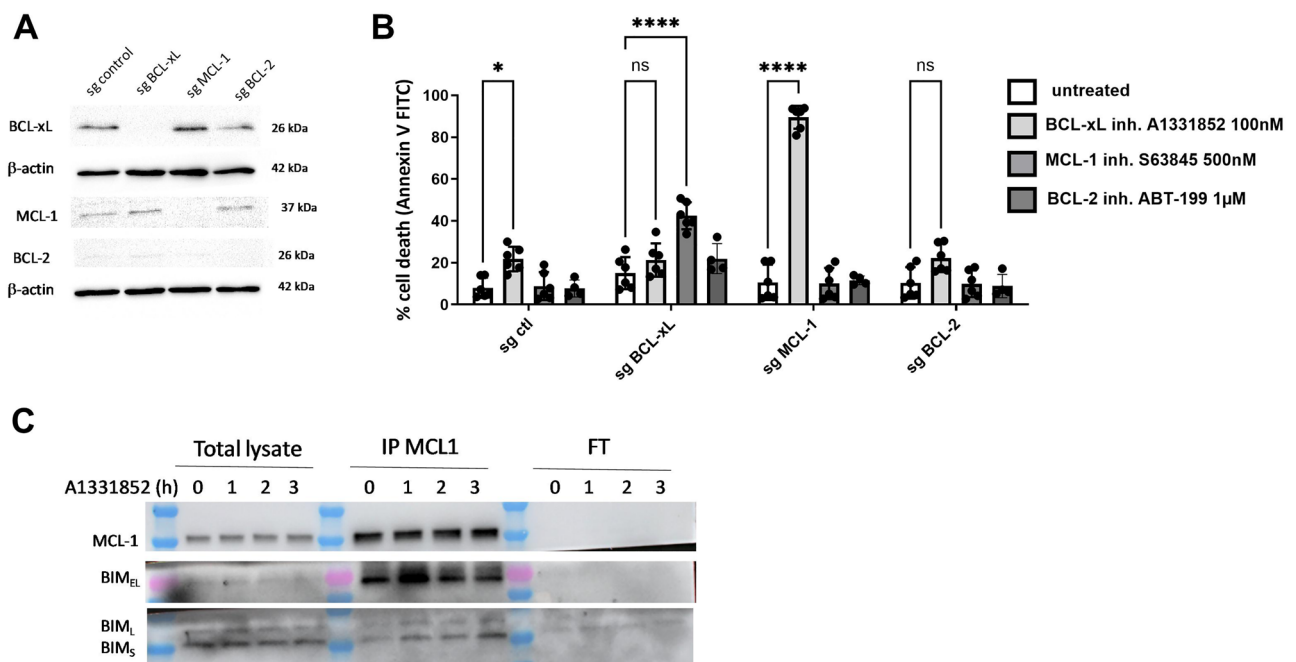


Figure 1. BCL-xL and MCL-1 are pivotal anti-apoptotic proteins responsible for the survival of the MDA-MB-231 cell line. **(A)** Validation of the downregulation of BCL-xL, MCL-1, and BCL-2 expression in engineered MDA-MB-231 cell line through western blot analysis. β -actin expression in the samples serves as a loading control. **(B)** Sensitivity of MDA-MB-231 deficient in MCL-1, BCL-xL or BCL-2 after a 48-h treatment with BH3 mimetics targeting these proteins (as indicated on the graph) in DMEM containing 0.5% FBS. Cell death is quantified by flow cytometry and the results are expressed as the percentage of cells labelled with annexin-V-FITC. Experiments were conducted in triplicate. P-values were determined by two-factor ANOVA, * $p \leq 0.05$, ** $p \leq 0.01$ and **** $p \leq 0.0001$. **(C)** Immunoprecipitation of MCL1 was performed after A1331852 treatment (100 nM) of MDA-MB-231 cells for the duration indicated (hour), followed by western blotting of BIM (FT: FlowThrough).

BCL-xL using A1331852¹⁴ resulted in cell death in MDA-MB-231. This outcome underscores the critical role of BCL-xL in the fundamental survival of these cells. To explore potential compensatory mechanisms between anti-apoptotic agents when inhibiting only one of them, we employed BH3 mimetics in the different anti-apoptotic-deficient cell lines. Inhibition of BCL-xL with A1331852 in MCL1-deficient cell line led to a substantial 90% cell death, suggesting that simultaneous targeting of both BCL-xL and MCL-1 is necessary to induce massive cell death. Conversely, pharmacological inhibition of MCL-1 by S63845¹⁵ in BCL-xL-deficient cell line resulted in a less pronounced cell death of only 40–50%. Inhibition of BCL-2 by ABT-199¹⁶ in BCL-xL or MCL-1-deficient MDA-MB-231 cells did not induce cell death compared to their respective controls. Similarly, pharmacological inhibition of BCL-xL or MCL-1 in MDA-MB-231 sg BCL-2 cells did not trigger cell death. Hence, BCL-2 does not play a significant role in the survival of MDA-MB-231 cells, consistent with their low expression of BCL-2. The increase in the cell death triggered by pharmacological blockade of MCL-1 when BCL-xL is absent differs from the one triggered by pharmacological inhibition of BCL-xL in cells where MCL-1 is suppressed. This difference could be attributed to variations in the binding levels of BCL-xL or MCL-1 with their pro-apoptotic partners. In fact, our results demonstrated an increase in the interaction between MCL-1 and the pro-apoptotic factor BIMs upon treatment with a BCL-xL antagonist (Fig. 1C), thus highlighting the readiness of MCL-1 to engage an extra apoptotic load (Fig. 1C).

In conclusion, our results highlight that BCL-xL and MCL-1 play significant roles in promoting the survival of MDA-MB-231 cell line. However, the inhibition of either BCL-xL or MCL-1 alone is insufficient to initiate a massive apoptotic response in this studied cancer line. The concomitant inhibition of BCL-xL and MCL-1 clearly increases cancer cells apoptosis, highlighting the presence of compensatory mechanisms between these two proteins.

BCL-xL significantly contributes to the resistance of the MDA-MB-231 cell line to chemotherapy

One standard of care for triple-negative breast cancers involves the combination of three chemotherapies: anthracycline (such as doxorubicin), alkylating agents (like cisplatin) and anti-metabolites (e.g., 5-fluorouracil). Combination of doxorubicin, cisplatin and 5-fluorouracil resulted in the death of only 25–30% of the MDA-MB-231 cell line as depicted in Fig. 2A. To identify the specific anti-apoptotic proteins responsible for impeding chemotherapy effectiveness in these cells, we employed CRISPR-Cas9 gene silencing and BH3 mimetics, as illustrated in Fig. 2B,C. Combining chemotherapy with the silencing of BCL-xL significantly increased cancer cell death from less than 20% to 60–70%, while silencing MCL-1 or BCL-2 had no substantial impact on sensitivity to chemotherapy (Fig. 2B). In accordance with this, combining chemotherapy with pharmacological inhibition of BCL-xL resulted in nearly 100% cell death, whereas MCL-1 inhibition had no effect (Fig. 2C). Contrary to BCL-2 silencing, the use of BH3 mimetics ABT-199 in combination with chemotherapy enhanced cell death to 60%, possibly due to an ABT-199 inhibitory effect on BCL-xL at the 1 μ M dose employed¹⁶. Indeed, the lower concentration of ABT-199 (100 nM) had no significant additional effect on chemotherapy-induced cell death (Fig. 2D). We confirmed the limiting effect of BCL-xL on the response to chemotherapy in BT-549, another triple-negative cell line, as we showed that only BCL-xL inhibitor significantly improved their response to chemotherapy (Fig. 2E).

To confirm the apoptotic nature of cell death induced by chemotherapy and BCL-xL inhibitor, we employed a pan-caspase inhibitor (Q-VD-OPh), as shown in Fig. 2F. In line with expectations, massive cell death induced by the combination of BH3 mimetics S63845 and A1331852 targeting MCL-1 and BCL-xL respectively was entirely blocked by Q-VD-OPh. Cell death induced by chemotherapy alone or in combination with BCL-xL inhibitor was reversed by Q-VD-OPh. This observation corroborates that cell death induced by chemotherapy, either alone or in combination with BCL-xL inhibitor, is apoptotic in nature.

In conclusion, BCL-xL plays a critical role in limiting the effectiveness of chemotherapy in the MDA-MB-231 cell line.

CAFs protect MDA-MB-231 cells from apoptosis triggered by simultaneous chemotherapy and BCL-xL silencing

Beyond their intrinsic resistance to chemotherapy, cancer cell survival may also be influenced by the surrounding tumor environment. Consequently, we explored how the presence of CAFs affects the susceptibility of MDA-MB-231 cells to apoptosis using a 2D coculture model. Our findings revealed that the presence of CAFs diminishes the apoptosis in MDA-MB-231 cells triggered by the combination of chemotherapeutic agents (Fig. 3A). Simultaneously, the response of CAFs to chemotherapy was variable, with CAF mortality ranging from 20 to 60% under chemotherapy conditions, and notably, the presence of MDA-MB-231 cells did not affect the sensitivity of CAFs to chemotherapy (Fig. 3B).

Since inhibiting BCL-xL makes cells more responsive to chemotherapy, we sought to determine whether CAFs could also counteract cell death induced by chemotherapy when BCL-xL was silenced. As illustrated in Fig. 3C, our results demonstrate that the presence of CAFs reverses the cell death triggered by the combination of chemotherapy and BCL-xL silencing. It is worth noting that the survival rate of BCL-xL deficient cells treated with chemotherapy under the influence of stromal pressure closely resembled that of control cancer cells treated with chemotherapy in monoculture (Fig. 3C). Concurrently, CAFs displayed variable responses to chemotherapy, and neither the presence of MDA-MB-231 control cells nor MDA-MB-231 cells with BCL-xL silencing influenced the sensitivity of CAFs to chemotherapy (Fig. 3D).

Hence, our findings emphasize that CAFs play a protective role against chemotherapy-induced apoptosis, even when the BCL-xL resistance factor is overcome in cancer cells.

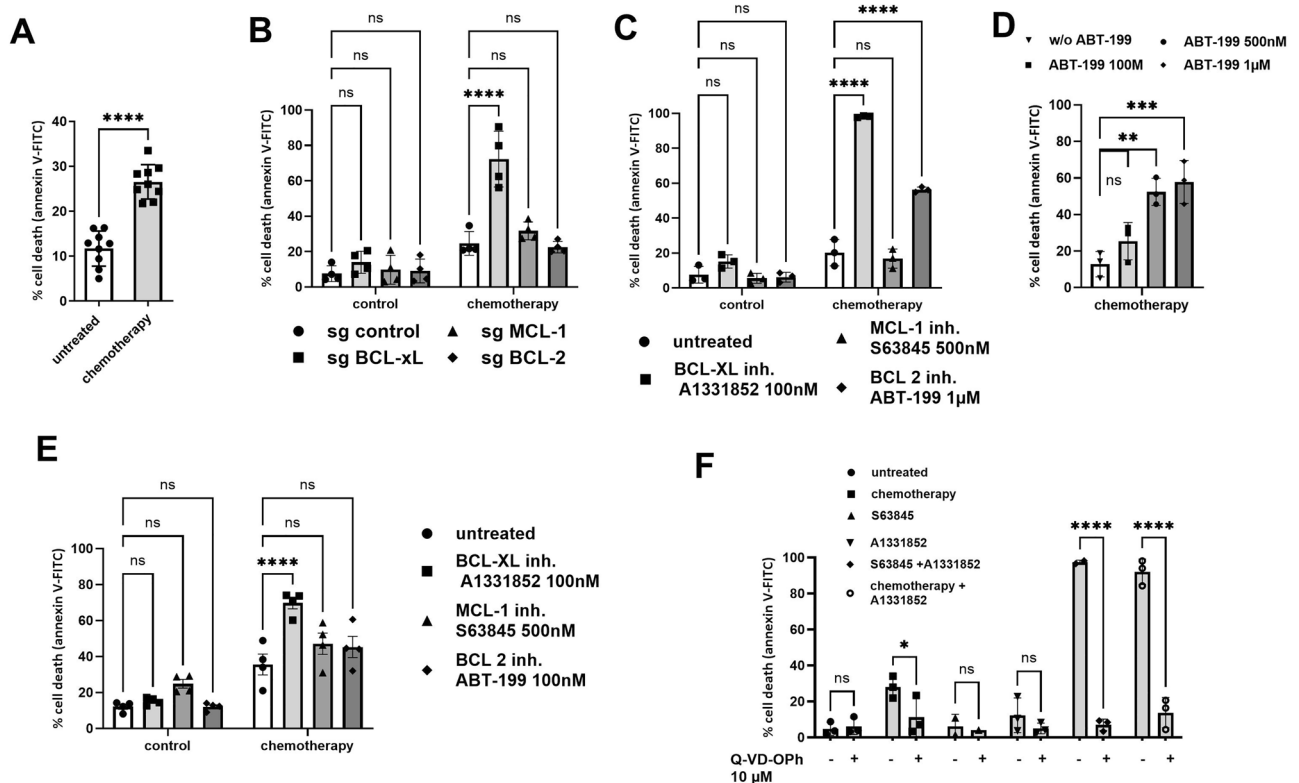


Figure 2. BCL-xL significantly contributes to the resistance of the MDA-MB-231 cell line to chemotherapy. (A) Sensitivity of MDA-MB-231 treated for 48 h with chemotherapy combining Doxorubicin (2.5 μM), 5-Fluorouracil (55 μM) and Cisplatin (27.5 μM). (B) Sensitivity of MDA-MB-231 cells silenced for anti-apoptotic proteins MCL-1, BCL-xL or BCL-2 to chemotherapy. (C) Sensitivity of MDA-MB-231 cells treated with chemotherapy combined to BH3 mimetics targeting BCL-xL, MCL-1 or BCL-2 (as indicated on the graph). (D) Sensitivity of MDA-MB-231 cells treated with chemotherapy combined to ABT-199 (100 nM, 500 nM or 1 μM). (E) Sensitivity of BT-549 cells treated with chemotherapy (Doxorubicin (1 μM), 5-Fluorouracil (22 μM) and Cisplatin (11 μM)) combined to BH3 mimetics targeting BCL-xL, MCL-1 or BCL-2 (as indicated on the graph) in RPMI1640 containing 1% FBS. (F) Sensitivity of MDA-MB-231 treated with different combinations of BH3 mimetics and chemotherapy in presence or not of Q-VD-Oph 10 μM . Cell death is quantified by flow cytometry. The results are expressed as the percentage of cells labelled with annexin-V-FITC. Experiments were conducted in triplicate. P-values were determined by two-factor ANOVA, * $p \leq 0.05$ and **** $p \leq 0.0001$.

BCL-xL expression is associated with patient-derived tumoroids responsiveness to chemotherapy

To investigate the responsiveness of primary human breast cancer cells to chemotherapy we used 7 breast cancer organoid cultures (hereinafter called tumoroids). Tumoroids derived from treatment naive breast cancer samples (Triple negative 1/7 cases (#2) and from luminal tumors in 6/7 cases) were grown ex vivo using a stem cell culture method¹⁷ that preserves mixtures of multiple tumor populations of flexible differentiation status^{18,19} (see Fig. 4A for microscopic analysis). We confirmed the epithelial origin of tumoroids by the expression of keratin 8 (Fig. 4C). It has been shown that culture conditions can influence the phenotype of cancer cells, modifying the expression of hormone receptors²⁰. Indeed, we showed in Fig. 4C that tumoroids did not express ER/PR hormone receptors in 5/7 cases. The level of Her2 expression appeared to be very low, confirming the non-amplified status of the original tumors (Fig. 4C). We assessed their response to chemotherapy via FACS analysis and identified variations in sensitivity among the tumoroids (Fig. 4B). In particular, tumoroids #2 and #5 showed greater sensitivity to chemotherapy than the other tumoroids, with high sensitivity as early as 0.5 μM of chemotherapy. In contrast, tumoroids #4, #6 and #7 were the less sensitive tumoroids to high dose of chemotherapy. Subsequently, we investigated the expression of BCL-xL, BCL-2 and MCL-1 in tumoroids using Western blot analysis of bulk lysates (Fig. 4C). Remarkably, while BCL-2 and MCL-1 expression appears relatively uniform we observed heterogeneity in BCL-xL expression within the tumoroids. Tumoroid #2, #3 and #5 displayed low levels of BCL-xL, while tumoroids #1, #4, #6 and #7 demonstrated high levels of BCL-xL. Tumoroids expressing the least BCL-xL are the most sensitive to chemotherapy (except tumoroid #3) and conversely the most resistant are those in which BCL-xL expression is high. There is in fact a negative correlation between sensitivity to 0.5 μM chemotherapy and the level of BCL-xL expression in tumoroids (Fig. 4D). We treated the most chemoresistant tumoroid (#4) with a combination of chemotherapy and BH3 mimetic antagonist of BCL-xL (A1331852, 100 nM). Consistent with our prior findings in resistant cancer cell line MDA-MB-231, the combination effectively reversed the resistance of

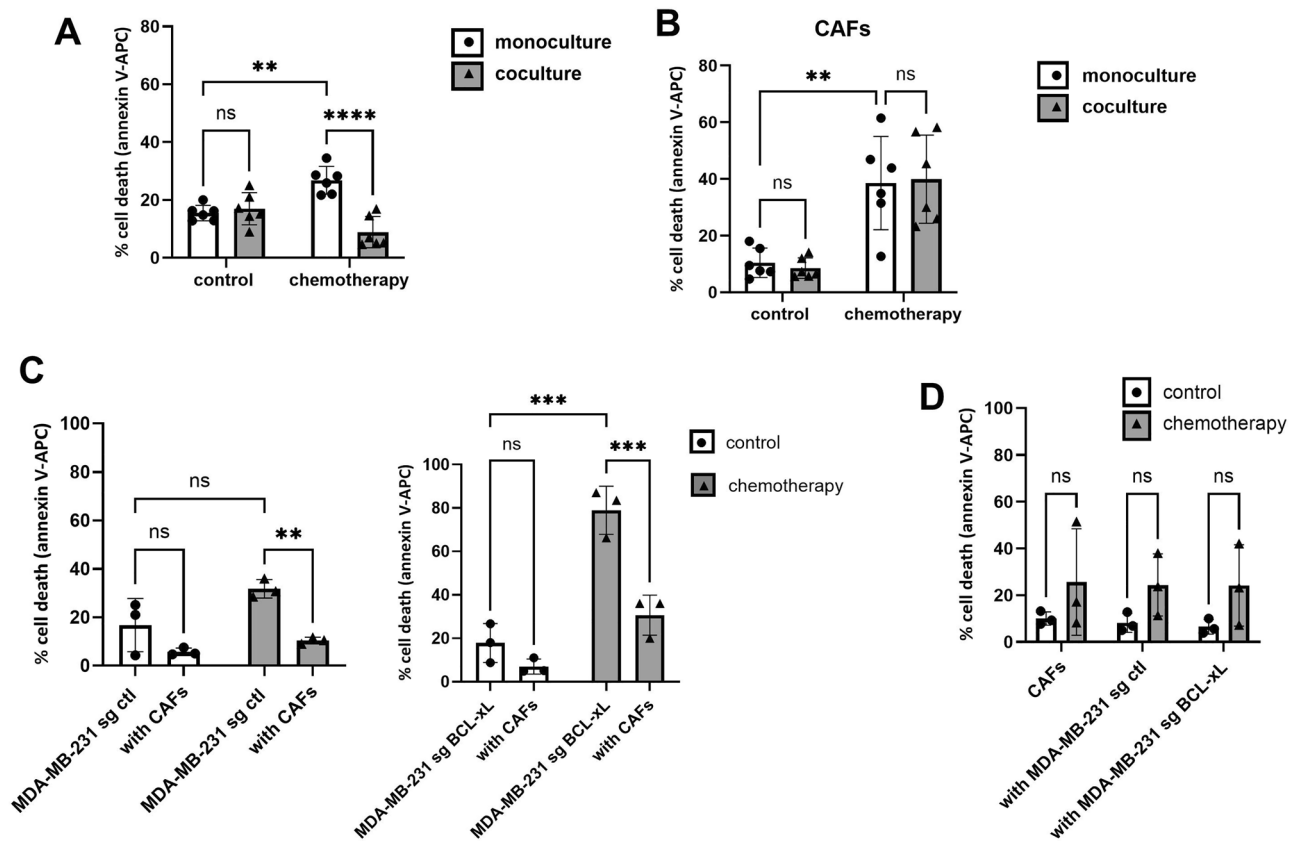


Figure 3. CAFs protect MDA-MB-231 cells from apoptosis triggered by simultaneous chemotherapy and BCL-xL silencing. **(A)** Sensitivity of MDA-MB-231 under chemotherapy in the absence or the presence of CAFs in 2D coculture. **(B)** Sensitivity of corresponding CAFs under chemotherapy in the absence or the presence of MDA-MB-231. **(C)** Sensitivity of MDA-MB-231 control (left) or deficient in BCL-xL (right) to chemotherapy in 2D coculture. **(D)** Sensitivity of corresponding CAFs under chemotherapy in the absence or the presence of MDA-MB-231 control or deficient in BCL-xL. Experiments were conducted in triplicate. P-values were determined by two-factor ANOVA, ** $p \leq 0.01$, *** $p \leq 0.001$ and **** $p \leq 0.0001$.

highly expressing BCL-xL tumoroid #4 (Fig. 4E). Consistently, A1331852 had no significant additional effect on chemotherapy sensitivity in tumors expressing low levels of BCL-xL (Fig. 4F). These findings indicate that BCL-xL expression and activity limit the chemosensitivity of patient-derived breast tumoroids. Finally, we observed that the most sensitive tumors (#2 and #5) were rendered more resistant to chemotherapy when treated in the presence of CAFs-conditioned media (Fig. 4G). This result confirms the impact of CAFs on cancer cells in tumoroid model of human breast cancer.

Discussion

In this study, we have demonstrated that triple negative breast cancer cells depend on the presence of BCL-xL and MCL-1 for their survival, which aligns with prior research findings^{21–23}. This finding aligns with a prior study, which demonstrated that targeting BCL-xL specifically with the BH3 mimetic enhanced the efficacy of docetaxel in a metastatic breast cancer xenograft model using MDA-MB-231 (LC3) cells¹⁴. To elaborate further, we investigated the impact of targeting various anti-apoptotic members within the BCL-2 family, namely, BCL-xL, MCL-1, and BCL-2, using a combination of drugs and gene silencing through CRISPR-Cas9 techniques. Our results revealed that the most effective approach for inducing cell death involved simultaneous inhibition of both MCL-1 and BCL-xL. However, it's worth noting that the outcome varied depending on the method used to target MCL-1 or BCL-xL individually. When we inhibited MCL-1 using the compound S63845 in cells lacking BCL-xL, the level of cell death observed was relatively moderate compared to when we pharmacologically targeted BCL-xL in cells where MCL-1 expression had been genetically removed. It has been previously described that the pro-apoptotic protein BIM shifts from one anti-apoptotic to the other to activate BAX and BAK and engage apoptosis²⁴. So, this discrepancy in cell death outcomes could potentially be attributed to differences in the initial binding of the pro-apoptotic protein BIM to either BCL-xL or MCL-1. Our results suggest that BCL-xL may be already and mostly engaged by a pro-apoptotic load (one or many pro-apoptotic effectors), while a significant portion of MCL-1 may be available to dynamically engage an extra apoptotic load. This might be explained by the rapid turnover of MCL-1 protein due to its short half-life, and by the fact that its binding by pro-apoptotic effectors fosters its turnover²⁵. Binding of BIM to MCL-1 increases under BCL-2 pharmacological inhibition in acute myeloid leukemia cells, thus emphasizing the ability of MCL-1 to take over pro-apoptotics released by other

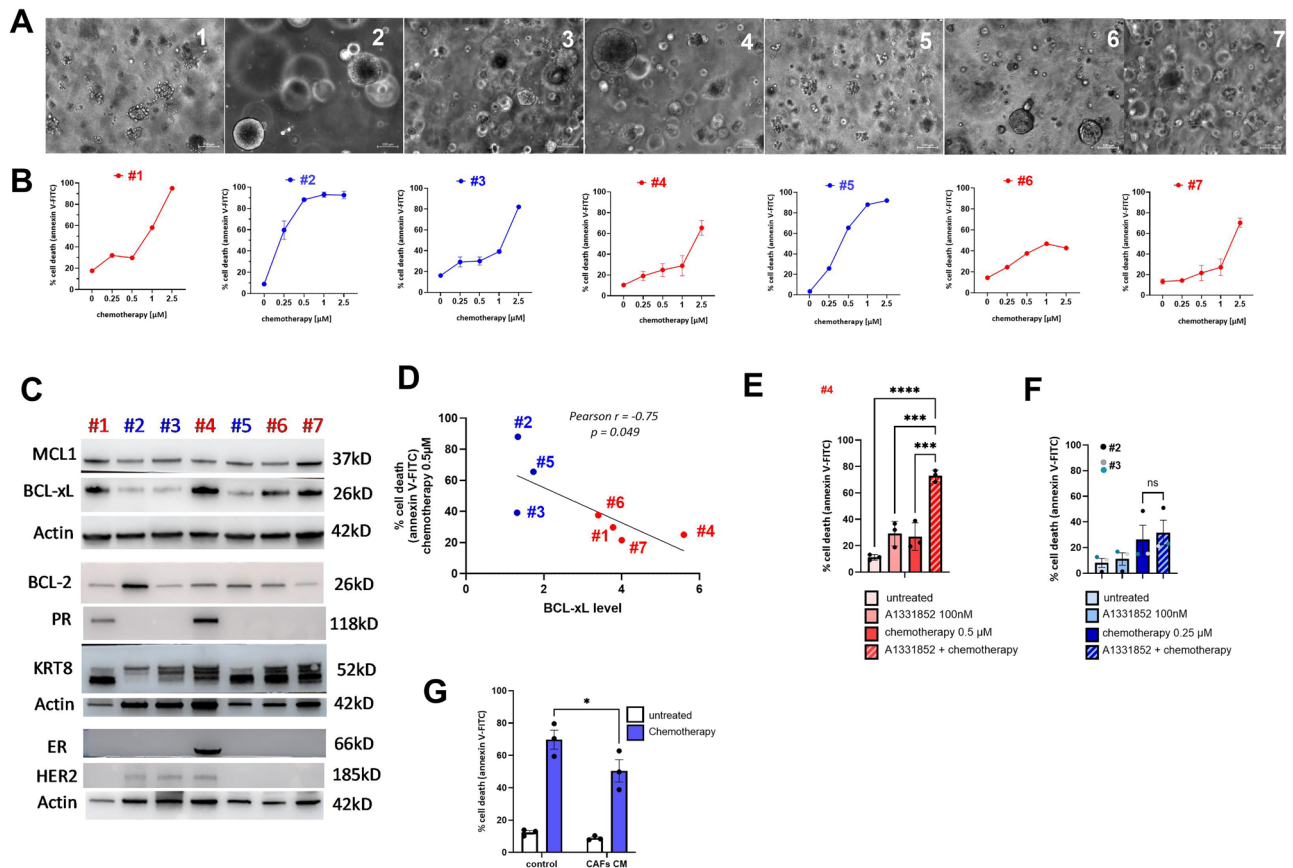


Figure 4. BCL-xL expression affects patient-derived tumoroids responsiveness to chemotherapy. (A) Illustration of treatment-naive-patient-derived tumoroids visualized by phase contrast microscopy. (B) Heterogeneous sensitivity of patient-derived tumoroids treated with chemotherapy combining Doxorubicin ($\times 1$), 5-Fluorouracil ($\times 22$) and Cisplatin ($\times 11$) for 48 h. The results are expressed as the percentage of cells labelled with annexin-V-FITC. Experiments were performed on 7 different tumoroids (#1 to #7). (C) Representative experiment of protein expression level of BCL-2 protein family members (MCL-1, BCL-2 and BCL-xL), hormone receptors (Estrogen Receptor: ER, Progesterone Receptor: PR and Human Epidermal Growth Factor Receptor-2: HER-2) and keratins (Keratin-8) in patient-derived tumoroids evaluated using western blots. β -actin expression is used as loading control. (D) Negative correlation (Pearson correlation coefficient $r = -0.75$; p value = 0.049) between percentage of cell death upon 0.5 μM chemotherapy for 48 h and BCL-xL levels determined by western-blot (relative to actin) in 7 organoids. (E) Sensitivity of tumoroid #4 to treatment of chemotherapy combined with BCL-xL antagonist: A1331852 (100 nM). The results are expressed as the percentage of cells labelled with annexin-V-FITC. (F) Sensitivity of tumoroid #2 ($n = 1$) and #5 ($n = 2$) to 0.25 and 0.5 μM chemotherapy respectively in the presence or not of CAFs conditioned media. The results are expressed as the percentage of cells labelled with annexin-V-FITC. P-values were determined by two-factor ANOVA, * $p \leq 0.05$, *** $p \leq 0.001$ and **** $p \leq 0.0001$.

anti-apoptotic proteins²⁶. In the same way, our results showed that pharmacological inhibition of BCL-xL led to an increased binding of BIM to MCL-1 (Fig. 1C). This underlies the significant role of MCL-1 in promoting “compensatory survival”, in response to an increase of free apoptotic effectors when BCL-xL is being targeted^{22,27}. It is interesting to note that our results also indicate a compensatory expression between BCL-xL and MCL-1 (Fig. 1A). Specifically, deletion of one of these proteins resulted in increased expression of the other.

Currently, aggressive breast cancers, comprising both triple-negative and luminal B subtypes, are primarily managed using conventional chemotherapy regimens that involve a combination of anthracyclines, alkylating agents, and antimetabolites^{28,29}. While combination therapies have improved treatment effectiveness in numerous instances, a subset of patients still exhibits resistance. To withstand chemotherapy, cancer cells employ various mechanisms, including inherent resistance to apoptosis governed by members of the BCL-2 family, as well as innate resistance factors like interactions with the extracellular matrix and the secretion of compounds into the tumor microenvironment³⁰. We demonstrate here that BCL-xL plays a crucial role in conferring inherent resistance to chemotherapy in cell line and primary breast cancer cells cultured in tumoroids. This underscores the importance of targeting BCL-xL in breast cancer treatment, especially when used in combination with current therapies. While specific BH3 mimetics designed to target BCL-xL have been developed, they pose a challenge due to on-target platelet toxicity, as platelets rely on BCL-xL for their survival^{31,32}. To address this issue, researchers have recently created PROTAC BCL-xL degraders, which recruit E3 ligases that are expressed at lower levels

in human platelets compared to various cancer cell lines^{33,34}. The approach of co-inhibiting BCL-xL alongside conventional therapies may offer a solution to counter the inherent resistance of cancer cells. However, our findings in MDA-MB-231 cells reveal that even when cancer cells become more responsive to chemotherapy due to BCL-xL inhibition, the presence of stromal CAFs nullifies this effect.

In a prior study, we elucidated that in cases of luminal breast cancer, CAFs possess the ability to diminish the sensitivity of cancer cells to apoptosis. This effect is primarily achieved by promoting the stabilization of MCL-1, mainly through the secretion of IL-6¹². The enhanced stabilization of MCL-1 makes these cancer cells more susceptible to MCL-1 targeting, a phenomenon previously observed in other models²¹. In our coculture model, it is possible that additional factors contribute to the resistance of cancer cells to BCL-xL inhibition induced by CAFs. CAFs have been shown to favor chemotherapy resistance in malignant cells via the secretion of growth factors, cytokines and matrix components, which modulate BCL-2 family proteins balance and also effectors of apoptosis downstream mitochondrial permeabilization such as survivin³⁵. CAFs could also protect malignant cells from apoptosis by modulating the nutrient context, what has already been shown previously in some studies³⁵. Additional investigation is required to determine the specific perturbations that CAFs induce in malignant cells within our model that might account for their protective effects.

With regard to the sensitivity of CAFs to apoptosis, we have previously shown that breast CAFs are primarily dependent on MCL-1 for survival and that in order to trigger effective apoptosis in these cells, it is necessary to jointly target MCL-1 and BCL-xL¹³. A promising strategy for targeting the protumoral effects of CAFs is to reverse their 'activated' phenotype. We have shown that targeting MCL-1 in CAFs attenuates their myofibroblastic phenotype, including a reduction in their pro-invasive capacity³⁶. In our study, CAFs protect BCL-xL deficient cancer cells against chemotherapy independently of their own sensitivity to treatments, which is heterogeneous. It has already been shown that the growth inhibition effect of conventional chemotherapy on CAFs from breast tumor patients is variable³⁷. The maintenance of CAF protective effect despite their disappearance suggests that CAFs could acquire an even more protective effect under chemotherapy. It has indeed already been shown that CAFs induce efficient chemoresistance in colorectal cancer-initiating cells when they are themselves exposed to the same conventional chemotherapy³⁸. Our results suggest that the strategy consisting in interrupting the dialog between CAFs and cancer cells could be more suitable than simply eliminating CAFs. It thus appears of particular interest to decipher mechanisms underlying protection from apoptosis induced by CAFs in malignant cells.

Our findings collectively suggest that, even when successfully addressing the inherent chemotherapy resistance mediated by BCL-xL, cancer-associated fibroblasts (CAFs) in the tumor microenvironment will still contribute to the development of acquired chemotherapy resistance. This underscores the need for interventions to overcome this additional obstacle to maximize the effectiveness of therapy.

Material and methods

Primary and cell lines culture

Fresh human mammary samples were obtained from treatment naive patients with breast carcinoma after surgical resection at the Institut de Cancérologie de l'Ouest, Nantes/Angers, France. Informed consent from enrolled patients was obtained as required by the French Committee for The Protection of Human Subjects, and Protocol was approved by Ministère de la Recherche (agreement no: DC-2012-1598) and by local ethic committee (agreement no: CB 2012/06).

To isolate CAFs from fresh samples, breast tissues were cut into small pieces in Dulbecco's Modified Eagle Medium (DMEM Thermo Fisher Scientific) supplemented with 10% FBS, 2 mM glutamine and 1% penicillin/streptomycin and placed in a plastic dish¹³. CAFs were isolated by their ability to adhere to plastic. After isolation, the fibroblasts were cultured in the same medium. Fibroblasts were used in the experiments before the ninth passage.

To isolate breast cancer cells from fresh samples, breast tissues were digested by collagenase (20 mg/ml) (Thermo Fisher) for 1h. Breast cancer tumoroids (50 000 cells in 120 μ L) were seeded in basement membrane extract (BME, BioTechne) in low adherence 24-well plates (Greiner) and cultured following the procedure previously described by Dekkers et al.²⁰. Briefly, Advanced DMEM/F12 was supplemented with penicillin/streptomycin, 10 mM HEPES, GlutaMAX (adDMEM/F12), 1X B27 (all Thermo Fisher), 1.25 mM *N*-acetyl-l-cysteine (Sigma-Aldrich), 10 mM nicotinamide (Sigma-Aldrich), 5 μ M Y-27632 (AbMole), 5 nM Heregulin β -1 (Peprotech), 500 nM A83-01 (Tocris), 5 ng/ml epidermal growth factor (Myltenyi), 20 ng/ml human fibroblast growth factor (FGF)-10 (Peprotech), Noggin (Myltenyi), Rspodin-1 (Milttenyi), 0.1 mg/ml primocin (Thermo Fisher), 1 μ M SB202190 (Sigma-Aldrich) and 5 ng/ml FGF-7 (Peprotech). The experiments were carried out on tumoroids between passages 4 and 10. For tumoroids treatment in presence of CAFs conditioned media (CAFs CM), CAFs CM were generated by adding 9 ml of tumoroid medium (Advanced DMEM/F12 as previously described except Y-27632 and A83-01) onto 100 mm dishes of $7-12 \times 10^5$ of CAFs. After 48h, CAFs CM were collected, centrifuged (2000g, 5 min) and supplemented with Y-27632 and A83-01 before being incubated with cancer cells with treatments for a further 48h before apoptosis analysis.

The human breast cell lines MDA-MB-231 and BT-549 were purchased from American Type Culture Collection (Bethesda, MD, USA). MDA-MB-231 cell line was cultured in DMEM supplemented with 5% FBS and 2 mM glutamine and BT-549 cell line was culture in RPMI-1640 medium supplemented with 10% FBS and 2 mM glutamine.

For the CRISPR Cas9-induced BCL-xL, MCL-1 or BCL-2 gene extinction, single guide (sg) RNA targeting human BCL-xL, MCL-1 or BCL-2 were designed using the CRISPR design tool (<http://crispor.tefor.net>). The following guide sequences were cloned in the lentiCRISPRV2 vector that was a gift from Feng Zhang (Addgene plasmid #52961): sg BCL-xL: 5'-GCAGACAGCCCCGCGGTGAA-3', sgMCL-1: 5'-CTGGAGACCTTACGACGGGT-3' and sg BCL-2: 5'-GAGAACAGGGTACGATAACC-3'. Empty vector was used as control. After

transduction, cells were selected using 1 µg/ml puromycin and protein extinctions were confirmed by immunoblot analysis. The experiments were conducted using deficient cells directly, without the need for establishing individual clones. All the cells are tested once a month to ensure they are mycoplasma-free.

Treatments

Doxorubicin (Selleckhem #S1208), Cisplatin (Selleckhem #S1166) and 5-Fluorouracil (Selleckhem #S1209) were mixed at 2.5 µM, 27.5 µM and 55 µM respectively to obtain chemotherapy treatment.

ABT-737 (Selleckhem #S1002), A1331852 (MedChemExpress #HY-19741), ABT-199 (ChimieTek #CT-A199), S63845 (ChimieTek #CT-S63845) and Q-VD-Oph (Sigma-Aldrich #SML0063) were used at indicated concentrations.

Coculture assays

Cell lines and primary CAFs co-culture was obtained by plating MDA-MB-231 with primary CAFs in monolayer with the ratio 1:3 in DMEM 10% FBS, 2 mM glutamine and 1% penicillin/streptomycin. After 24 h, the co-culture was maintained in DMEM 1% FBS, 2 mM glutamine and 1% penicillin/streptomycin for additional 24 h. Treatments were then added as indicated for 48 h. Mono-cultures (MDA-MB-231 or CAFs) were performed in the same conditions as controls.

Apoptosis assay

Cell death was assessed using an Annexin-V FITC binding assay (Miltenyi #130-092-052) performed according to manufacturer's instructions. Flow-cytometry analysis was performed on Accuri C6 Plus flow cytometer from BD Biosciences. For co-culture apoptosis assay, cell suspension was stained with FITC-conjugated human CD90 antibody (BD Biosciences #555595) prior to Annexin-V APC binding assay (BD Biosciences #550474) according to manufacturer's instructions.

Immunoblot analysis

Cells were resuspended in lysis buffer (RIPA, Thermo-Fisher #98901). After sodium dodecyl sulfate–polyacrylamide gel electrophoresis (SDS-PAGE), proteins (20 µg per condition) were transferred to a 0.45 µM nitrocellulose membrane (Trans-Blot Turbo RTA Transfer kit nitrocellulose midi #1704271) using Trans-Blot Turbo Transfer System (Bio-Rad #1704150, parameters: 25 V, 1A, 30 min). The membrane was then blocked with 5% non-fat milk TBS 0.05% Tween 20 for 1 h at room temperature and incubated with primary antibody overnight at 4 °C. The used primary antibodies were: anti-BCL-xL (abcam #ab32370), anti-MCL-1 (Cell Signaling #94296), anti-BCL-2 (abcam #ab117115), anti-ER (abcam #ab16660), anti-PR (abcam #ab32085), anti-Her2 (ThermoFischer #PA5-14635), anti-Keratin8 (abcam #ab53280) and anti-β-actin (EMD Millipore #MAB1501). The membrane was then incubated with appropriate HRP-conjugated secondary antibody (Jackson Immuno-Research Laboratories, Goat anti-Rabbit #111-035-006 or Goat anti-Mouse #115-035-006) for 1 h at room temperature and visualization was made using the Fusion FX from Vilber (Eberhardzell, Deutschland).

Co-Immunoprecipitation

Cells were collected in lysis buffer (CHAPS 1%, TRIS-HCl 20mM pH = 7.5, NaCl 150mM, EDTA 1mM pH = 8.0, proteases and phosphatases inhibitors). Co-Immunoprecipitation was performed using PureProteome™ Protein A Magnetic Beads (Millipore, LSKMAGA10). Protein extracts were first precleared using 10µl of beads for 200µg of proteins (1-h incubation at 4 °C). 2µl of anti-MCL-1 antibody (Cell signaling mAb #94296) and 10µl of beads were then used for 200 µg of proteins following manufacturer's instructions. For western blotting, BIM antibody (Sigma, AB17003) was used as primary antibody (1:1000) and the same anti-MCL-1 primary antibody (1:1000). Clean-Blot™ IP Detection Reagent (HRP) (Thermo Scientific #21230) was used as secondary antibody (1:1000).

Statistical analysis

Two-way analysis of variance (ANOVA) was used for statistical analysis for overall condition effects with Graph-Pad Prism 10.2 Software. All data are presented as mean +/- SD of at least three independent experiments.

Ethics approval and consent to participate

Informed consent was obtained from enrolled patients and protocol was approved by Ministère de la Recherche (agreement no: DC-2012-1598) and by local ethic committee (agreement no: CB 2012/06). All experiments were performed in accordance with relevant guidelines and regulations.

Data availability

Data supporting the results of this study are available from the corresponding author, F. S., upon reasonable request.

Received: 1 March 2024; Accepted: 12 June 2024

Published online: 19 June 2024

References

- Burstein, H. J. *et al.* Customizing local and systemic therapies for women with early breast cancer: the St. Gallen International Consensus Guidelines for treatment of early breast cancer 2021. *Ann. Oncol.* **32**, 1216–1235. <https://doi.org/10.1016/j.annonc.2021.06.023> (2021).

2. Howlader, N., Cronin, K. A., Kurian, A. W. & Andridge, R. Differences in breast cancer survival by molecular subtypes in the United States. *Cancer Epidemiol. Biomark. Prev. Publ. Am. Assoc. Cancer Res. Cosponsored Am. Soc. Prev. Oncol.* **27**, 619–626. <https://doi.org/10.1158/1055-9965.EPI-17-0627> (2018).
3. Hannun, Y. A. Apoptosis and the dilemma of cancer chemotherapy. *Blood* **89**, 1845–1853. <https://doi.org/10.1182/blood.V89.6.1845> (1997).
4. Juin, P., Geneste, O., Gautier, F., Depil, S. & Campone, M. Decoding and unlocking the BCL-2 dependency of cancer cells. *Nat. Rev. Cancer* **13**, 455–465. <https://doi.org/10.1038/nrc3538> (2013).
5. Yip, K. W. & Reed, J. C. Bcl-2 family proteins and cancer. *Oncogene* **27**, 6398–6406. <https://doi.org/10.1038/onc.2008.307> (2008).
6. Goodwin, C. M., Rossanese, O. W., Olejniczak, E. T. & Fesik, S. W. Myeloid cell leukemia-1 is an important apoptotic survival factor in triple-negative breast cancer. *Cell Death Differ.* **22**, 2098–2106. <https://doi.org/10.1038/cdd.2015.73> (2015).
7. Olopade, O. I. *et al.* Overexpression of BCL-x protein in primary breast cancer is associated with high tumor grade and nodal metastases. *Cancer J. Sci. Am.* **3**, 230–237 (1997).
8. Petrocca, F. *et al.* A genome-wide siRNA screen identifies proteasome addiction as a vulnerability of basal-like triple-negative breast cancer cells. *Cancer Cell* **24**, 182–196. <https://doi.org/10.1016/j.ccr.2013.07.008> (2013).
9. Delbridge, A. R. D. & Strasser, A. The BCL-2 protein family, BH3-mimetics and cancer therapy. *Cell Death Differ.* **22**, 1071–1080. <https://doi.org/10.1038/cdd.2015.50> (2015).
10. Castells, M., Thibault, B., Delord, J.-P. & Couderc, B. Implication of tumor microenvironment in chemoresistance: tumor-associated stromal cells protect tumor cells from cell death. *Int. J. Mol. Sci.* **13**, 9545–9571. <https://doi.org/10.3390/ijms13089545> (2012).
11. Sahai, E. *et al.* A framework for advancing our understanding of cancer-associated fibroblasts. *Nat. Rev. Cancer* **20**, 174–186. <https://doi.org/10.1038/s41568-019-0238-1> (2020).
12. Su, S. *et al.* CD10+GPR77+ cancer-associated fibroblasts promote cancer formation and chemoresistance by sustaining cancer stemness. *Cell* **172**, 841–856.e16. <https://doi.org/10.1016/j.cell.2018.01.009> (2018).
13. Louault, K. *et al.* Interactions between cancer-associated fibroblasts and tumor cells promote MCL-1 dependency in estrogen receptor-positive breast cancers. *Oncogene* **38**, 3261–3273. <https://doi.org/10.1038/s41388-018-0635-z> (2019).
14. Levenson, J. D. *et al.* Exploiting selective BCL-2 family inhibitors to dissect cell survival dependencies and define improved strategies for cancer therapy. *Sci. Transl. Med.* **7**, 279ra40. <https://doi.org/10.1126/scitranslmed.aaa4642> (2015).
15. Kotschy, A. *et al.* The MCL1 inhibitor S63845 is tolerable and effective in diverse cancer models. *Nature* **538**, 477–482. <https://doi.org/10.1038/nature19830> (2016).
16. Souers, A. J. *et al.* ABT-199, a potent and selective BCL-2 inhibitor, achieves antitumor activity while sparing platelets. *Nat. Med.* **19**, 202–208. <https://doi.org/10.1038/nm.3048> (2013).
17. Sachs, N. *et al.* A living biobank of breast cancer organoids captures disease heterogeneity. *Cell* **172**, 373–386.e10. <https://doi.org/10.1016/j.cell.2017.11.010> (2018).
18. Bhatia, S. *et al.* Patient-derived triple-negative breast cancer organoids provide robust model systems that recapitulate tumor intrinsic characteristics. *Cancer Res.* **82**, 1174–1192. <https://doi.org/10.1158/0008-5472.CAN-21-2807> (2022).
19. Uematsu, H. *et al.* De-differentiation in cultures of organoids from luminal-type breast cancer is restored by inhibition of NOTCH signaling. *Hum. Cell* <https://doi.org/10.1007/s13577-023-00975-7> (2023).
20. Dekkers, J. F. *et al.* Long-term culture, genetic manipulation and xenotransplantation of human normal and breast cancer organoids. *Nat. Protoc.* **16**, 1936–1965. <https://doi.org/10.1038/s41596-020-00474-1> (2021).
21. Campbell, K. J. *et al.* Breast cancer dependence on MCL-1 is due to its canonical anti-apoptotic function. *Cell Death Differ.* <https://doi.org/10.1038/s41418-021-00773-4> (2021).
22. Campbell, K. J. *et al.* MCL-1 is a prognostic indicator and drug target in breast cancer. *Cell Death Dis.* **9**, 19. <https://doi.org/10.1038/s41419-017-0035-2> (2018).
23. Levenson, J. D. *et al.* Potent and selective small-molecule MCL-1 inhibitors demonstrate on-target cancer cell killing activity as single agents and in combination with ABT-263 (navitoclax). *Cell Death Dis.* **6**, e1590. <https://doi.org/10.1038/cddis.2014.561> (2015).
24. Alcon, C. *et al.* ER+ breast cancer strongly depends on MCL-1 and BCL-xL anti-apoptotic proteins. *Cells* **10**, 1659. <https://doi.org/10.3390/cells10071659> (2021).
25. Adams, K. W. & Cooper, G. M. Rapid turnover of Mcl-1 couples translation to cell survival and apoptosis. *J. Biol. Chem.* **282**, 6192–6200. <https://doi.org/10.1074/jbc.M610643200> (2007).
26. Bhatt, S. *et al.* Reduced mitochondrial apoptotic priming drives resistance to BH3 mimetics in acute myeloid leukemia. *Cancer Cell* **38**, 872–890.e6. <https://doi.org/10.1016/j.ccell.2020.10.010> (2020).
27. Montero, J. *et al.* Destabilization of NOXA mRNA as a common resistance mechanism to targeted therapies. *Nat. Commun.* <https://doi.org/10.1038/s41467-019-12477-y> (2019).
28. Hassan, M. S. U., Ansari, J., Spooner, D. & Hussain, S. A. Chemotherapy for breast cancer (review). *Oncol. Rep.* **24**, 1121–1131. <https://doi.org/10.3892/or.00000963> (2010).
29. Won, K.-A. & Spruck, C. Triple-negative breast cancer therapy: Current and future perspectives (review). *Int. J. Oncol.* **57**, 1245–1261. <https://doi.org/10.3892/ijo.2020.5135> (2020).
30. Senthilane, D. A. *et al.* The role of tumor microenvironment in chemoresistance: To survive, keep your enemies closer. *Int. J. Mol. Sci.* **18**, 1586. <https://doi.org/10.3390/ijms18071586> (2017).
31. Mason, K. D. *et al.* Programmed anuclear cell death delimits platelet life span. *Cell* **128**, 1173–1186. <https://doi.org/10.1016/j.cell.2007.01.037> (2007).
32. Vlahovic, G. *et al.* A phase I safety and pharmacokinetic study of ABT-263 in combination with carboplatin/paclitaxel in the treatment of patients with solid tumors. *Investig. New Drugs* **32**, 976–984. <https://doi.org/10.1007/s10637-014-0116-3> (2014).
33. Khan, S. *et al.* BCL-XL PROTAC degrader DT2216 synergizes with sotorasib in preclinical models of KRASG12C-mutated cancers. *J. Hematol. Oncol.* **15**, 23. <https://doi.org/10.1186/s13045-022-01241-3> (2022).
34. He, Y. *et al.* Using proteolysis-targeting chimera technology to reduce navitoclax platelet toxicity and improve its senolytic activity. *Nat. Commun.* **11**, 1996. <https://doi.org/10.1038/s41467-020-15838-0> (2020).
35. Nocquet, L., Juin, P. P. & Souazé, F. Mitochondria at center of exchanges between cancer cells and cancer-associated fibroblasts during tumor progression. *Cancers* **12**, 3017. <https://doi.org/10.3390/cancers12103017> (2020).
36. Bonneaud, T. L. *et al.* Targeting of MCL-1 in breast cancer-associated fibroblasts reverses their myofibroblastic phenotype and pro-invasive properties. *Cell Death Dis.* **13**, 787. <https://doi.org/10.1038/s41419-022-05214-9> (2022).
37. Sonnenberg, M. *et al.* Highly variable response to cytotoxic chemotherapy in carcinoma-associated fibroblasts (CAFs) from lung and breast. *BMC Cancer* **8**, 364. <https://doi.org/10.1186/1471-2407-8-364> (2008).
38. Lotti, F. *et al.* Chemotherapy activates cancer-associated fibroblasts to maintain colorectal cancer-initiating cells by IL-17A. *J. Exp. Med.* **210**, 2851–2872. <https://doi.org/10.1084/jem.20131195> (2013).

Acknowledgements

We thank members of the “Stress adaptation and tumor escape” laboratory for their support. We benefited from technical support from the Cytometry Core facility (CytoCell) of Nantes University. L. Nocquet was a recipient of French ministry of Higher Education, Research and Innovation and was supported by a fellowship from Ligue

contre le *cancer* (CD44). This work was supported by INCa (SIRIC ILIAD INCa-DGOS INSERM-ITMO Cancer-18011 and PLBIO021-129NN), and departmental committee of LIGUE Contre le Cancer CD44, CD53 and CD22. P.P.J.'s laboratory is labeled by the Ligue Nationale Contre le Cancer (LNCC). P.P.J. acknowledges the Association Ruban Rose for providing support.

Author contributions

L.N., J. R., C.C.L., L.D. and F.S. conducted experiments. L.N., P.P.J. and F.S. designed the experiments. L.N., P.P.J. and F.S. analyzed the data. M.C. gave assistance in collecting tissue samples. L.N., P.P.J. and F.S. wrote the paper. P.P.J. and F.S. obtained funding. P.P.J. and F.S. conceived the study and supervised it. All authors contributed to the article and approved the submitted version.

Competing interests

The authors declare no competing interests.

Additional information

Supplementary Information The online version contains supplementary material available at <https://doi.org/10.1038/s41598-024-64696-z>.

Correspondence and requests for materials should be addressed to P.P.J. or F.S.

Reprints and permissions information is available at www.nature.com/reprints.

Publisher's note Springer Nature remains neutral with regard to jurisdictional claims in published maps and institutional affiliations.



Open Access This article is licensed under a Creative Commons Attribution 4.0 International License, which permits use, sharing, adaptation, distribution and reproduction in any medium or format, as long as you give appropriate credit to the original author(s) and the source, provide a link to the Creative Commons licence, and indicate if changes were made. The images or other third party material in this article are included in the article's Creative Commons licence, unless indicated otherwise in a credit line to the material. If material is not included in the article's Creative Commons licence and your intended use is not permitted by statutory regulation or exceeds the permitted use, you will need to obtain permission directly from the copyright holder. To view a copy of this licence, visit <http://creativecommons.org/licenses/by/4.0/>.

© The Author(s) 2024